# Detecting triplet locking by triplet synchronization indices

Björn Kralemann,[1] Arkady Pikovsky,[2] and Michael Rosenblum[2]

[1]*Institut für Pädagogik, Christian-Albrechts-Universität zu Kiel, Olshausenstrasse 75, 24118 Kiel, Germany*
[2]*Institute of Physics and Astronomy, University of Potsdam, Karl-Liebknecht-Strasse 24/25, 14476 Potsdam-Golm, Germany*

We discuss the effect of triplet synchrony in oscillatory networks. In this state the phases and the frequencies of three coupled oscillators fulfill the conditions of a triplet locking, whereas every pair of systems remains asynchronous. We suggest an easy to compute measure, a triplet synchronization index, which can be used to detect such states from experimental data.

## I. INTRODUCTION

Synchronization of self-sustained oscillatory systems is a fundamental nonlinear phenomenon, extensively studied within the last 3 decades [1]. Being weakly coupled, systems of this class tend to adjust their frequencies and phases. This happens because the direction along the flow of the dynamical system in its state space is neutrally stable and therefore susceptible to even a very small perturbation or interaction. Since the neutrally stable direction corresponds to the phase of the oscillator, its phase and hence its frequency can be easily shifted due to a weak coupling to other systems.

In spite of essential progress made, synchronization remains a topic of interest in numerous theoretical and experimental studies and finds various applications, in particular, in analysis of oscillatory time series [2–5]. There are two basic approaches to this data analysis problem. In one formulation, one tries to recover a description of the interaction between two self-sustained oscillators from the time series, e.g., via reconstruction of the coupling function in the phase approximation [6]. Recent attempts [7] are aimed at extension of this approach to cover the oscillator networks, e.g., to analyze the interaction of respiratory, cardiac, and brain activities [8]. In another approach one does not reconstruct the underlying equations but focuses on establishing synchronization features by analyzing some correlation between the signals or their phases [2,9,10]. Quite popular here is the so-called synchronization index, also called the phase locking value (see, e.g., [11]), which can be computed even for noisy and nonstationary time series, provided the phases are extracted from the available signals.

Our main goal in this paper is to extend this analysis to more complex synchronization patterns in multifrequency systems. Such an approach naturally calls for incorporation of the theoretical results on the synchronization of multifrequency systems (see, e.g., [12] for an analysis of external synchronization of the van der Pol oscillator with a modulated natural frequency, [13] for studies of mutual synchronization of electronic three-dimensional quasiperiodic systems, and [14] for numerical and experimental investigations of forced and mutual synchronization of quasiperiodic oscillators with two basic frequencies). In a general formulation [15], synchronization of systems with $N > 2$ basic frequencies can be understood as the occurrence of resonances on an $N$-dimensional torus. Although this basic feature is well known, to our knowledge this concept has never been applied to quantification of high-order synchrony in oscillator networks

from multivariate data. In this paper we exploit this concept and suggest a simple measure which reliably detects triplet synchrony from time series.

This paper is organized as follows. In Sec. II we briefly discuss triplet locking, and in Sec. III we introduce the corresponding synchronization index. In Sec. III we present the numerical results, which are then discussed in Sec. V.

## II. TRIPLET SYNCHRONY

In the simplest setup, two limit-cycle oscillators (or an oscillator and a driving force) are said to be $n : m$ synchronized if the conditions of phase and frequency locking,

$$|n\varphi_1 - m\varphi_2| < \text{const}, \quad n\Omega_1 - m\Omega_2 = 0, \tag{1}$$

are fulfilled. Here $\varphi_{1,2}$ are the oscillators' phases, $\Omega_{1,2} = \langle \dot\varphi_{1,2} \rangle$ are the observed frequencies of interacting systems, $m$ and $n$ are some positive integers, and $\langle \cdot \rangle$ denotes time averaging. Due to an interaction, the observed frequencies $\Omega_{1,2}$ generally differ from the frequencies of autonomous oscillators (natural frequencies) $\omega_{1,2}$. It is important that conditions (1) are fulfilled in a finite range of the detuning $\omega_1 - \omega_2$. Synchronization can also be described in geometrical terms: while the image of the asynchronous, quasiperiodic motion is a two-dimensional torus (spanned by the two phases) in the phase space of the coupled systems, the transition to synchrony corresponds to an appearance of a stable limit cycle on this torus; this picture is valid for at least not very strong coupling.

A larger number of interacting oscillators ($N > 2$) generally builds a network. Now, depending on the distribution of the natural frequencies, on the network structure, and on the coupling parameters, different dynamical regimes are possible [16]. Full phase locking is observed when conditions (1) are valid for any pair of units; correspondingly, the dynamics in the phase space of the system of $N$ oscillators reduces to a stable limit cycle on the $N$-dimensional torus (spanned by $N$ phases). It may happen that some pairs of oscillators synchronize, while they remain asynchronous with the rest of the network. In this context one speaks of partial synchrony [17], when the dynamics reduces to a stable torus of a dimension between 1 and $N$. Furthermore, oscillators can form several synchronous groups (clusters), so that every pair within the cluster is synchronized according to (1); clusters can coexist with an asynchronous group. These types of synchrony are usually tackled by a pairwise analysis of phase and frequency locking according to Eq. (1). However, pairwise analysis may not
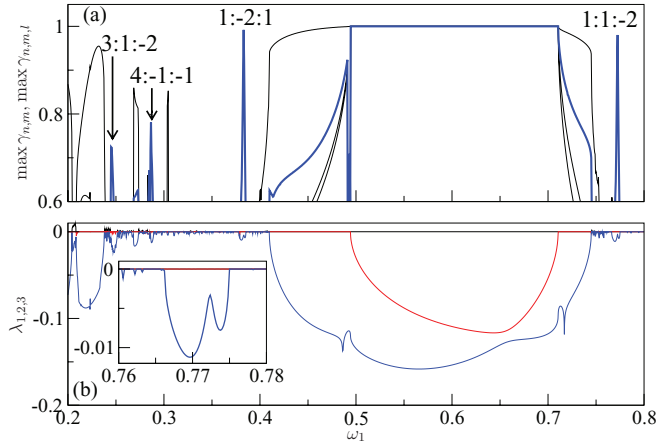
FIG. 1. (Color online) (a) Pairwise synchronization indices (black solid line) and triplet index (thick blue line). There are four domains where the triplet index is large whereas pairwise indices are small; this indicates the triplet locking. (The order of the locking is shown on the plot, e.g., 3:1:−2 means that the triplet index maximizes for $n = 3$, $m = 1$, and $l = −2$.) The large domain $0.5 \lesssim \omega_1 \lesssim 0.7$ is a domain of complete synchronization (all three oscillators are locked). (b) Three largest Lyapunov exponents of the coupled system (lines); negative values indicate phase locking. A small parameter range around $\omega_1 \approx 0.77$, where triplet locking 1:1:−2 is observed, is magnified in the inset.

reveal all synchronous states of a network because, generally, we expect to observe high-order resonances on the tori.

For definiteness, we fix $N = 3$. Here, in addition to usual pairwise locking described by Eq. (1), we expect to find a synchronous state, when *triplets* of oscillators adjust their phases and frequencies so that the following conditions are fulfilled:

$$|n\varphi_1 + m\varphi_2 + l\varphi_3| < \text{const}, \quad n\Omega_1 + m\Omega_2 + l\Omega_3 = 0, \quad (2)$$

where integers $n, m, l$ can be both positive and negative, while the conditions of the pairwise synchrony equation (1) are *not* satisfied for any pair of units. We denote this state as *triplet synchrony*.

It is instructive to discuss the triplet and the pairwise synchronies in terms of Lyapunov exponents (LE). When the systems are uncoupled, the spectrum contains three zero LEs, corresponding to the phases of the oscillators, and negative LEs, describing the transverse stability of the limit cycles (their number depends on the dimensionality of oscillator subsystems). The negative exponents are practically unaffected by the coupling and are not important for the following discussion, while the initially zero LEs reflect synchronization transitions. If one pair of oscillators gets frequency locked while the third one remains asynchronous, one zero LE becomes negative and two remain zero. Locking of all three oscillators is characterized by one zero LE. When three oscillators are locked in a triplet, the three phases are subject to the stable condition (2), and therefore one zero LE becomes negative. Thus, the spectra of LEs do not distinguish between the triplet synchrony and the state when one pair of oscillators is synchronized. In terms of the phase space, both the triplet and the pair synchrony correspond to a two-dimensional torus in the three-dimensional space of three phases. The difference

is that for the pairwise synchrony the torus lies "parallel" to one of the axes [see Fig. 2(a) below], while for the triplet synchrony it lies "diagonally" [see Fig. 2(b) below].

## III. TRIPLET SYNCHRONIZATION INDEX

In a numerical or physical experiment where one can vary or control the oscillators' natural frequencies, the triplet synchrony can easily be detected by directly checking the locking conditions, (1) and (2), depending on these parameters (cf. Fig. 3 below). In experimental studies, where only short time series from the interacting systems are available and the oscillators are inevitably noisy, one typically quantifies the degree of interrelation between the phases by some correlation measure, e.g., by means of the $n : m$ synchronization index, or the phase locking value [2,11]:

$$\gamma_{n,m} = |\langle e^{i(n\varphi_1 - m\varphi_2)} \rangle|. \quad (3)$$

Here $n$ and $m$ are integers which are typically chosen by trial so that the index is maximized. The index is close to 1 in the case of the pairwise locking described by condition (1) and zero otherwise. (Notice that even in the case of perfect synchronization, $\gamma_{n,m}$ is generally less than 1 due to possible oscillations of the generalized phase difference $n\varphi_1 - m\varphi_2$ around some mean value.)

If $N > 2$ interacting oscillators build a network, then the synchronous states are usually characterized via the pairwise analysis as well, namely, by computation of indices (3) for all pairs. Naturally, the triplet-synchronous states are not revealed by this analysis. Therefore, we introduce a triplet synchronization index:

$$\gamma_{n,m,l} = |\langle e^{i(n\varphi_1 + m\varphi_2 + l\varphi_3)} \rangle|, \quad (4)$$

which quantifies whether the phases of three oscillators fulfill condition (2). In case of a perfect locking, $n\varphi_1 + m\varphi_2 + l\varphi_3 = \text{const}$, the index $\gamma_{n,m,l} \approx 1$, while it is zero if at least two of the three phases are completely independent; intermediate values, $0 < \gamma_{n,m,l} < 1$, are observed when the oscillators undergo a transition from autonomous to synchronized dynamics. Below we demonstrate that the proposed quantity efficiently reveals triplet-synchronous states. Furthermore, we show that
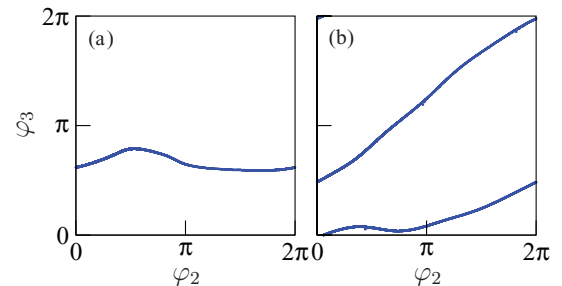


FIG. 2. (Color online) Trajectories on the three-dimensional torus. Poincaré maps for $\varphi_1 = 0$ are shown for (a) $\omega_1 = 0.72$ and (b) $\omega_1 = 0.77$. In (a), for fixed $\varphi_1$ the variation of $\varphi_3$ is small, which means that $\varphi_3 - \varphi_1 \approx \text{const}$, while $\varphi_2$ attains all values in the range $[0, 2\pi)$; this is a sign of synchronization between oscillators 1 and 3, while oscillator 2 is asynchronous. In (b), for fixed $\varphi_1$, both phases $\varphi_{2,3}$ vary from zero to $2\pi$, remaining, however, in a functional relationship; this is an example of a triplet-synchronous state.
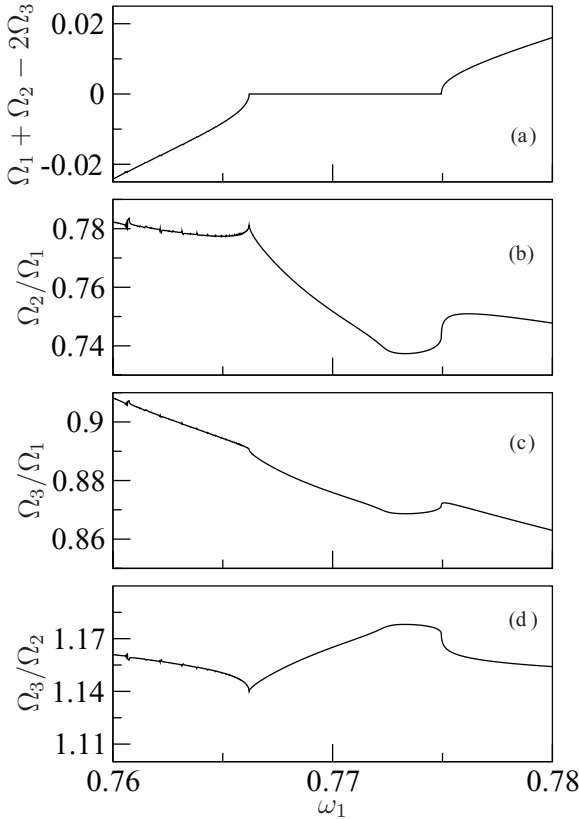
FIG. 3. (a) Illustration of the triplet locking condition $\Omega_1 + \Omega_2 - 2\Omega_3 = 0$. (b)–(d) Absence of pairwise locking.

triplet-synchronous states appear already in a quite standard setup with pairwise linear diffusive coupling of oscillators.

## IV. NUMERICAL EXAMPLE

Our basic model is a ring of three coupled Rayleigh oscillators [18]:

$$\ddot{x}_1 - \mu\left(1 - \dot{x}_1^2\right)\dot{x}_1 + \omega_1^2 x_1 = \varepsilon(\dot{x}_3 + \dot{x}_2 - 2\dot{x}_1),$$
$$\ddot{x}_2 - \mu\left(1 - \dot{x}_2^2\right)\dot{x}_2 + \omega_2^2 x_2 = \varepsilon(\dot{x}_3 + \dot{x}_1 - 2\dot{x}_2), \quad (5)$$
$$\ddot{x}_3 - \mu\left(1 - \dot{x}_3^2\right)\dot{x}_3 + \omega_3^2 x_3 = \varepsilon(\dot{x}_1 + \dot{x}_2 - 2\dot{x}_3).$$

In the first numerical experiment we fixed parameters $\mu = 0.5$, $\omega_2 = 0.52$, $\omega_3 = 0.65$, and $\varepsilon = 0.1$, whereas frequency $\omega_1$ was varied between 0.2 and 0.8 with a step of 0.0005. The system was integrated with the fourth-order Runge-Kutta method with a time step of 0.02.

For each set of frequencies we computed the LEs and the synchronization indices. For this goal, we first obtained, for all oscillators, the protophases

$$\theta_{1,2,3} = \arctan\left(-\frac{\dot{x}_{1,2,3}}{\omega_{1,2,3} x_{1,2,3}}\right) \quad (6)$$

and then performed a transformation to phases, $\theta \to \varphi$ (see [6]). This step is necessary because the protophases, although they yield correct observed frequencies, are not uniformly distributed in the interval $[0, 2\pi)$, and therefore the synchronization index calculated using variables $\theta$ will not vanish even in the absence of the coupling. The transformation to the

phases, according to [6], is performed as follows: (i) we find the probability densities of the protophases $\rho_i(\theta_i)$, and (ii) we obtain the genuine phases according to $\varphi = 2\pi \int_0^\theta \rho(\theta') \, d\theta'$. Notice that this is a reversible transformation, not a filter, so that no information is lost in this step. Then the phases $\varphi_i$ are used to calculate indices (3) and (4).

In this way, for all values of $\omega_1$ we obtained three pairwise indices $\gamma_{n,m}^{(1,2)}$, $\gamma_{n,m}^{(2,3)}$, and $\gamma_{n,m}^{(1,3)}$ for $n, m \leqslant 5$ and took their maximal values; the superscripts here correspond to the oscillator indices. Next, we computed the maximal, over all combinations with $|n|, |m|, |l| \leqslant 5$, triplet index $\gamma_{n,m,l}$. The results, shown in Fig. 1(a), indicate four domains of triplet locking of different orders. Within these domains the triplet index is large while the pairwise indices are small. (Notice that for all indices $0 \leqslant \gamma \leqslant 1$.) The variation of LEs with $\omega_1$ is consistent with the calculated indices [Fig. 1(b)]: large values of indices correspond to negative LEs. However, as discussed above, the distinction between pairwise and triplet locking on the basis of LEs is not possible. This is illustrated in Fig. 2, where we present Poincaré maps of the three-dimensional torus for two cases, $\omega_1 = 0.72$ and $\omega_1 = 0.77$. (The sections are constructed by taking $\varphi_1 = 0$.) In both cases the triplet index is large, $\gamma_{1,1,-2} > 0.8$. However, in the first case one pairwise index is large as well, whereas in the second case all pairwise indices are much smaller than $\gamma_{1,1,-2}$. The Poincaré maps confirm that the cases $\omega_1 = 0.72$ and $\omega_1 = 0.77$ correspond to the pairwise and the triplet lockings, respectively.

Figure 3 presents the details for the domain of the 1:1:−2 locking. Here we show that condition (2) is fulfilled while the natural frequency $\omega_1$ is varied in a finite range [19]. Thus, the high value of the triplet index revealed a true locked state, not an occasional coincidence of frequencies.

For the case of triplet locking, it is natural to represent the synchronization regions as domains in the three-dimensional parameter space spanned by $\omega_1 - \omega_3$, $\omega_2 - \omega_3$, and $\varepsilon$. This is illustrated for the case of the 1:1:−2 locking in Fig. 4. Here we show four cross sections of the parameter space for four values of the coupling strength and for constant $\omega_3 = 0.65$ (therefore we use $\omega_1, \omega_2$ as the coordinates). Different domains (no locking, pairwise locking, full synchrony, and triplet locking) are shown by gray scales. Naturally, the domain of triplet locking is stretched along the line $\omega_1 + \omega_2 = 1.3 = 2\omega_3$. This stripe connects the domains of pairwise and/or full synchrony. Notice that the stripe becomes wider, but shorter, as the coupling strength $\varepsilon$ increases. Indeed, on the one hand, an increase in coupling facilitates triplet locking, but on the other hand, the domains of the usual (pairwise and/or full) locking may grow even faster with $\varepsilon$, and in the parameter space no place for the triplet locking remains.

In the second numerical experiment we checked how frequent the triplet states are (cf. [15]). For this goal we performed about $8 \times 10^4$ runs with the natural frequencies $\omega_{1,2,3}$ randomly chosen from the interval [0.5, 1.5]. For each run we computed the observed frequencies $\Omega_{1,2,3}$ (by following the phase growth for each oscillator over the large time interval $2.5 \times 10^4$; see also [19]) and checked the conditions of pairwise and triplet locking [see Eqs. (1) and (2), respectively] for $n, m, |l| \leqslant 20$. The condition was considered fulfilled if $|n\Omega_1 + m\Omega_2 + l\Omega_3| \leqslant 10^{-4}$. Simultaneously, we counted the number of zero LEs; practically, we attributed
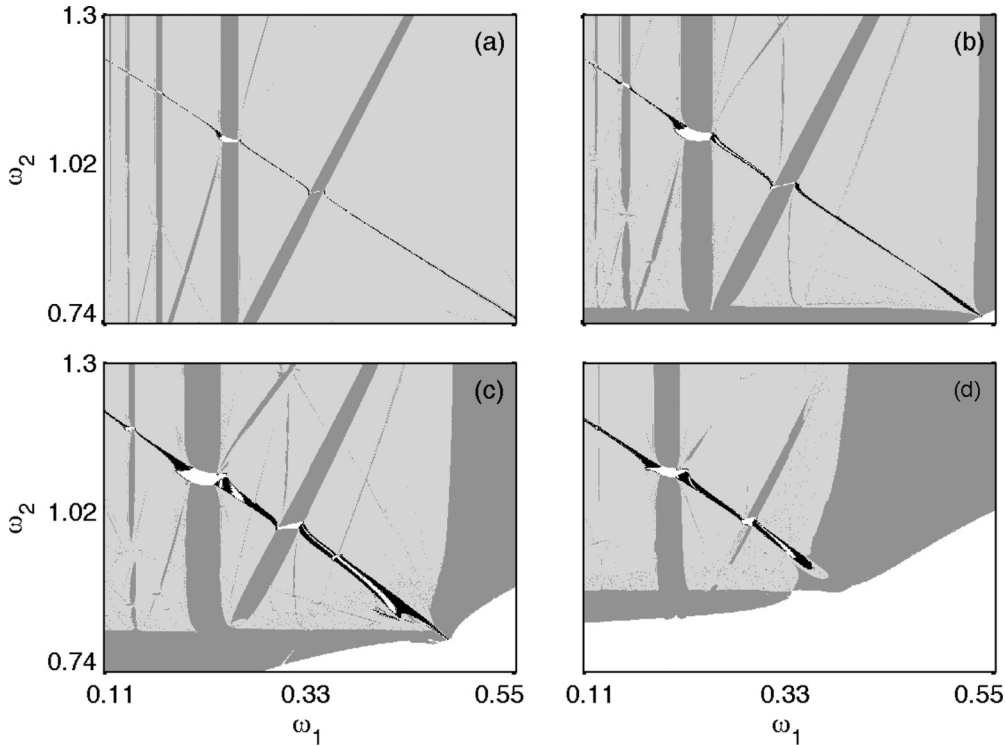
FIG. 4. Synchronization regions of order $1:1:-2$ for (a) $\varepsilon = 0.05$, (b) $\varepsilon = 0.1$, (c) $\varepsilon = 0.15$, and (d) $\varepsilon = 0.2$. Triplet locking, full synchrony, and pairwise locking are shown by black, white, and dark gray, respectively. Asynchronous states are presented by light gray.

the LEs satisfying $|\lambda| \leqslant 10^{-5}$ as zero ones (this threshold depends on the length of the numerical run). The results for five different values of the coupling strength $\varepsilon$ are shown in Fig. 5. Here we show only the relative probability of different synchronous states. For small couplings, the most probable are synchronous states with pair synchrony; for large couplings, the most probable are those with full synchrony. Triplet synchrony appears with a probability of a few percent. In the chosen frequency range, the most "popular" resonant combination of frequencies is $2\Omega_1 = \Omega_2 + \Omega_3$ (with a proper

permutation); such triplets represent $\approx 40\%$ of all observed triple resonances for moderate couplings and about $80\%$ for the largest coupling $\varepsilon = 0.2$. Not shown in the diagram are quasiperiodic states, which dominate for small couplings (they occur with probabilities of $60\%$, $50\%$, $41\%$, $25\%$, and $10\%$ for couplings $\varepsilon = 0.05$, $0.075$, $0.1$, $0.15$, $0.2$, respectively). Chaotic states are very rare (maximal occurrence of $0.25\%$ for $\varepsilon = 0.15$).

## V. DISCUSSION

In this paper we have suggested a simple technique to detect the triplet synchrony in the oscillator networks from the observed data. Although the triplet synchrony is known from the theory, we believe that it was important to demonstrate that such regimes are not exotic and can naturally appear in a heterogeneous network, in particular in experiments with large groups of oscillators of different origins, e.g., mechanical, electronic, chemical, etc. [20]. We expect that triplet indices (4), due to their simplicity, will become a common tool in data analysis. Possible applications are the quantification of the coordination of respiratory, cardiac, and brain activities [8] and of the interaction of different brain regions, where oscillations with a hierarchy of frequencies are ubiquitous [21]. Furthermore, the concept of triplet synchronization might contribute to research in neuroscience based on the binding-by-synchrony hypothesis [22], which states that synchronized patterns of neural activity constitute cognitive related content since complex forms of synchronization might correspond to more complex forms of cognitive binding.
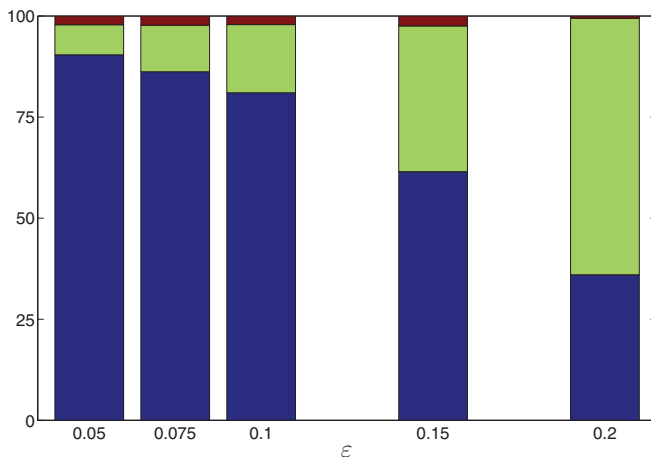


FIG. 5. (Color online) The relative frequency of different synchronous states (percent) for model (6) with randomly chosen frequencies. From bottom to top: pairwise synchrony, full synchrony, and triplet synchrony.

The proposed measure can easily be extended to reveal quadruplets and higher-order resonances in networks of more than three units. However, we expect the corresponding parameter domains to be very narrow and the probability of observing such states from noisy data to be very small. Nevertheless, complex synchronous states can naturally arise. Indeed, suppose as an example that three elements of a large network build a triplet $n\omega_1 + m\omega_2 + l\omega_3 = 0$ and also that one of these elements synchronizes with another oscillator, so that, e.g., $k\omega_3 = p\omega_4$. Then oscillators 1, 2, and 4 also fulfill the condition of triplet locking, $nk\omega_1 + mk\omega_2 + lp\omega_3 = 0$.

Finally, we mention that a high value of the index $\gamma$ demonstrates a high degree of interrelation between the phases, and in spite of the commonly used name "synchronization index," it only indicates possible synchronization and does not prove its existence (for the latter a determination of the locking region, like in Fig. 3, is required). Generally, a high value of $\gamma$ can be due to other types of interaction, e.g., due to modulation. All the problems in interpretation of the pairwise analysis by means of $\gamma$ remain relevant in case of triplets. Similarly, like in the pairwise analysis, the problem of statistical significance can be tackled by surrogate data tests [23]. Preliminary calculations performed for the case illustrated in Fig. 3 show that triplet synchrony can be clearly distinguished from the usual one if the time series contain at least ten oscillation periods. Detailed analysis of the statistical properties of index estimation and of the effect of dynamical and measurement noises remains a subject for future studies.

[1] Y. Kuramoto, *Chemical Oscillations, Waves and Turbulence* (Springer, Berlin, 1984); A. Pikovsky, M. Rosenblum, and J. Kurths, *Synchronization: A Universal Concept in Nonlinear Sciences* (Cambridge University Press, Cambridge, 2001); S. H. Strogatz, *Sync: The Emerging Science of Spontaneous Order* (Hyperion, New York, 2003); S. C. Manrubia, A. S. Mikhailov, and D. H. Zanette, *Emergence of Dynamical Order: Synchronization Phenomena in Complex Systems*, Lecture Notes in Complex Systems, Vol. 2 (World Scientific, Singapore, 2004).

[2] M. G. Rosenblum, A. S. Pikovsky, J. Kurths, C. Schäfer, and P. A. Tass, in *Neuro-informatics and Neural Modeling*, edited by F. Moss and S. Gielen, Handbook of Biological Physics, Vol. 4 (Elsevier, Amsterdam, 2001), pp. 279–321.

[3] N. B. Janson, A. G. Balanov, V. S. Anishchenko, and P. V. E. McClintock, Phys. Rev. E **65**, 036211 (2002); **65**, 036212 (2002).

[4] M. G. Rosenblum, A. S. Pikovsky, and J. Kurths, Fluctuation Noise Lett. **4**, L53 (2004); M. G. Rosenblum, L. Cimponeriu, and A. S. Pikovsky, in *Handbook of Time Series Analysis*, edited by B. S. M. Winterhalder and J. Timmer (Wiley-VCH, Weinheim, 2006), pp. 159–180.

[5] K. Lehnertz, Physiol. Meas. **32**, 1715 (2011).

[6] M. G. Rosenblum and A. S. Pikovsky, Phys. Rev. E **64**, 045202 (2001); J. Miyazaki and S. Kinoshita, Phys. Rev. Lett. **96**, 194101 (2006); I. T. Tokuda, S. Jain, I. Z. Kiss, and J. L. Hudson, *ibid.* **99**, 064101 (2007); B. Kralemann, L. Cimponeriu, M. Rosenblum, A. Pikovsky, and R. Mrowka, Phys. Rev. E **77**, 066205 (2008).

[7] B. Kralemann, A. Pikovsky, and M. Rosenblum, Chaos **21**, 025104 (2011); A. Duggento, T. Stankovski, P. V. E. McClintock, and A. Stefanovska, Phys. Rev. E **86**, 061126 (2012).

[8] B. Musizza, A. Stefanovska, P. V. E. McClintock, M. Paluš, J. Petrovčič, S. Ribarič, and F. Bajrović, J. Physiol. **580**, 315 (2007).

[9] P. Tass, M. G. Rosenblum, J. Weule, J. Kurths, A. Pikovsky, J. Volkmann, A. Schnitzler, and H.-J. Freund, Phys. Rev. Lett. **81**, 3291 (1998); R. Q. Quiroga, A. Kraskov, T. Kreuz, and P. Grassberger, Phys. Rev. E **65**, 041903 (2002).

[10] B. Schelter, M. Winterhalder, R. Dahlhaus, J. Kurths, and J. Timmer, Phys. Rev. Lett. **96**, 208103 (2006); M.

Wickramasinghe and I. Z. Kiss, Phys. Rev. E **83**, 016210 (2011); J. Sun, Z. Li, and S. Tong, Comput. Math. Methods Med. (2012) 239210.

[11] J.-P. Lachaux, E. Rodriguez, J. Martinerie, and F. J. Varela, Human Brain Mapping **8**, 194 (1999); F. Mormann, K. Lehnertz, P. David, and C. E. Elger, Phys. D **144**, 358 (2000); T. Kreuz, Scholarpedia **6**, 11922 (2011).

[12] P. S. Landa and N. D. Tarankova, Radio Eng. Electron. Phys. **21**, 34 (1976); P. S. Landa, *Nonlinear Oscillations and Waves in Dynamical Systems* (Kluwer, Dordrecht, 1996).

[13] A. P. Kuznetsov, S. P. Kuznetsov, and N. V. Stankevich, Commun. Nonlinear Sci. Numer. Simul. **15**, 1676 (2010); A. Kuznetsov, S. Kuznetsov, E. Seleznev, and N. Stankevich, in *Nonlinear Dynamics of Electronic Systems* (VDE-Verlag, Berlin Offenbach, 2012), pp. 100–102.

[14] V. Anishchenko, S. Nikolaev, and J. Kurths, Phys. Rev. E **73**, 056202 (2006); **76**, 046216 (2007).

[15] C. Grebogi, E. Ott, and J. A. Yorke, Phys. D **15**, 354 (1985).

[16] M. Barahona and L. M. Pecora, Phys. Rev. Lett. **89**, 054101 (2002); I. V. Belykh, V. N. Belykh, and M. Hasler, Phys. D **195**, 188 (2004); Y. Moreno and A. F. Pacheco, Europhys. Lett. **68**, 603 (2004); E. Barreto, B. Hunt, E. Ott, and P. So, Phys. Rev. E **77**, 036107 (2008); A. Arenas, A. Diaz-Guilera, and C. J. Perez-Vicente, Phys. Rev. Lett. **96**, 114102 (2006).

[17] E. A. Martens, E. Barreto, S. H. Strogatz, E. Ott, P. So, and T. M. Antonsen, Phys. Rev. E **79**, 026204 (2009).

[18] The Rayleigh equation can be obtained from the van der Pol equation with the help of the variable substitution $x/\sqrt{3} \to \dot{x}$. Our choice of the model is purely technical: the limit cycle of the Rayleigh oscillator is closer to a circle, which simplifies numerical estimation of the phase.

[19] For computation of observed frequencies $\Omega_k$, $k = 1,2,3$, we integrate, along with the equations of the system, three instantaneous frequencies $\dot{\theta}_k = \omega_k \frac{\dot{x}_k^2 - \ddot{x}_k \dot{x}_k}{\omega_k^2 x_k^2 + \dot{x}_k^2}$ [cf. Eq. (6)]. In this way we obtain the unwrapped protophases $\theta_k$ and compute $\Omega_k = [\theta_k(T) - \theta_k(0)]/T$, where $T$ is the integration time.

[20] G. Heinrich, M. Ludwig, J. Qian, B. Kubala, and F. Marquardt, Phys. Rev. Lett. **107**, 043603 (2011); A. A. Temirbayev,

Z. Z. Zhanabaev, S. B. Tarasov, V. I. Ponomarenko, and M. Rosenblum, Phys. Rev. E **85**, 015204 (2012); M. Zhang, G. S. Wiederhecker, S. Manipatruni, A. Barnard, P. McEuen, and M. Lipson, Phys. Rev. Lett. **109**, 233906 (2012); M. R. Tinsley, S. Nkomo, and K. Showalter, Nat. Phys. **8**, 662 (2012); E. A. Martens, S. Thutupalli, A. Fourrière, and O. Hallatschek, arXiv:1301.7608.

[21] G. Buzsáki, *Rhythms of the Brain* (Oxford University Press, Oxford, 2006).

[22] P. M. Milner, Psychol. Rev. **81**, 521 (1974); C. M. Gray, P. König, A. K. Engel, and W. Singer, Nature (London) **338**, 334 (1989); C. von der Malsburg, Neuron **24**, 95 (1999); A. Revonsuo, Consciousness Cognition **8**, 173 (1999).

[23] H. Kantz and T. Schreiber, *Nonlinear Time Series Analysis*, 2nd ed. (Cambridge University Press, Cambridge, 2004); M. Palus and D. Hoyer, IEEE Eng. Med. Biol. Mag. **17**, 40 (1998); A. Schmitz, Phys. Rev. E **62**, 7508 (2000); K. T. Dolan and A. Neiman, *ibid*. **65**, 026108 (2002).